

# Formation of Multilayered Ti–Hf–Si–N/NbN/Al<sub>2</sub>O<sub>3</sub> Coatings with High Physical and Mechanical Properties

A.D. POGREBNJAK<sup>a,\*</sup>, M.S. PROZOROVA<sup>b</sup>, M.G. KOVALYOVA<sup>b</sup>, O.V. KOLISNICHENKO<sup>c</sup>,  
V.M. BERESNEV<sup>d</sup>, K. OYOSHI<sup>e</sup>, Y. TAKEDA<sup>e</sup>, A.S. KAVERINA<sup>a</sup>, A.P. SHYPPYLENKO<sup>a</sup>  
AND J. PARTYKA<sup>f</sup>

<sup>a</sup>Sumy State University, R. Korsakov 2, 40007 Sumy, Ukraine

<sup>b</sup>Belgorod State University, Belgorod, Russia

<sup>c</sup>Paton Welding Institute NAS of Ukraine, Kiev, Ukraine

<sup>d</sup>National Kharkov University, Kharkov, Ukraine

<sup>e</sup>National Institute for Material Science, Tsukuba, Japan

<sup>f</sup>Lublin University of Technology, Nadbystrzycka 38a, 20-618 Lublin, Poland

This work presents the first results on forming of multi-layered superhard coatings Ti–Hf–Si–N/NbN/Al<sub>2</sub>O<sub>3</sub> and their properties as well as structure. Microstructure, elemental and phase compositions of multi-layered coatings obtained by different methods were investigated. There were used such methods as: scanning electron microscopy EDS JEM-7000F microscope (with microanalysis) for research of cross-section of coatings, with subsequent Auger-electron spectroscopy, X-ray diffraction analysis, optical inverted microscope Olympus GX51, electron-ion microscopes Quanta 200 3D and Quanta 600 (scanning electron microscopy), equipped by the detector of X-ray radiation of the system PEGASUS 2000. It was stated that hardness of coatings has reached 56 GPa, and at the same time the factor of wearing during friction was the smallest —  $2.571 \times 10^{-5}$ . It was also noted that nitrogen pressure in the chamber at the deposition of the top layer significantly influences on the properties of samples. For example, the coefficient of friction at  $P = 0.3$  Pa from 0.2 at the beginning of track to 0.001 (during the tests), and at the pressure of nitrogen  $P = 0.8$  Pa, the coefficient of friction was equal to 0.314 at the beginning of track and 0.384 at the end (during the tests).

DOI: [10.12693/APhysPolA.123.813](https://doi.org/10.12693/APhysPolA.123.813)

PACS: 41.75.–i, 61.80.–x, 81.15.–z

## 1. Introduction

Multicomponent, multi-layered and nanostructured coatings are currently the basis for the implementation of the protection of devices for different functional purposes [1–4]. It is well known that the ceramic coating Al<sub>2</sub>O<sub>3</sub> exhibits high resistance to corrosive and oxidizing environments, as well as provides protection for the parts operating at high temperatures [5]. In [1, 2] it was shown that the multi-layer coating of Ti–Al–N/Ti–N/Al<sub>2</sub>O<sub>3</sub>, obtained by different techniques provides good protection against corrosion and wear, and is resistant to temperatures up to 900 °C. However, the increase of annealing temperature in air to over 950 °C leads to oxidation of multicomponent coating. Therefore, the development of a new generation of multi-layer nano- and microstructured coatings of high physical-mechanical and tribological properties to increase the range of protective functions is an important task of solid state physics.

To obtain Al<sub>2</sub>O<sub>3</sub> coatings the two-chambered hollow-detonation device consisting of cylindrical and annular chambers, coupled with the barrel, which is applied to heat and accelerate the powder-dispersed materials, was used. Initiation of a gas mixture (propane, oxygen, air)

was performed under the frequency of 20 Hz, which provided a quasi-continuous mode of operation of the device with the constant transfer of powder to the heating and acceleration zone [5]. The coatings were deposited using AMPERIT<sup>®</sup>R740.0 Al<sub>2</sub>O<sub>3</sub> powder with the main fraction of 5.6–22.6 μm (about 5% of the powder particles have a characteristic size  $\geq 50$  μm). For the next deposition of coatings, the cathodic vacuum arc deposition with HF stimulation was applied, with the cathodes of N and Ti–Hf–Si. The potential bias and residual pressure in the chamber were varied during the experiment. Nitrogen gas was used for the formation of nitrides. Thus, the thickness of the Al<sub>2</sub>O<sub>3</sub> coating was 180 μm, thickness of the NbN sublayer was about 1.2 μm, and the thickness of the layer (Ti–Hf–Si)N ranged from 5 to 12 μm.

The study of the microstructure and elemental composition of the coatings was carried out using several raster electron-ion microscopes (Quanta 200 3D, Quanta 600 SEM), glow discharge spectrometer GD-Profilier 2<sup>TM</sup>. Depth profile analysis is a continuous process of sputtering through a sample at a rate of typically 3 μm per min. Equipped with X-ray detector system PEGASUS 2000 and JEOL-7000F (Japan). The microhardness measurements were carried out on the microsection surface and the substrate by using an automatic system for the analysis of DM-8 microhardness with a load on the indenter 25 and 300 g by the Vickers method. The porosity of coatings was determined by metallography with el-

\*corresponding author; e-mail: [alexpi@i.ua](mailto:alexpi@i.ua)

ements of qualitative and quantitative analysis of pore geometry using an optical inverted microscope Olympus GX51. The structure and phase composition of coatings were obtained by the XRD grazing incidence analysis in Cr radiation on the set up Rigaku RINT-2500-MDG.

Measurements of nanohardness and elastic modulus were carried out by Nanaoindenter II (USA) with the Berkovich pyramid. A tribological study was performed using the scratch tester REVETEST (CSM Instruments), which measured the friction coefficient  $\mu$ , the factor of wear, and acoustic emission during indentation of the pyramid Rokwell-C.

Since the coating has a well-definable interface with the substrate, the main parameter for determining the quality of the coating is free from defects at the coating/substrate interface. The studies found that the apparent surface of adhesion of  $Al_2O_3$  coating to the substrate is free of defects, i.e. the areas with weak bonds (micro-cracks) located in one plane, which are able to spread applying external loads.

**2. Results and discussion**

The surface of the microsection of the interface coating/substrate was etched with an alcoholic solution of nitric acid. The active constituents of the material boundaries dissolved, and the cross-section shows that in the zone of contact with the substrate coating has a mixed structure (Fig. 1a) consisting of the islands of coating of very different shapes and sizes in steel envelope. The main elements of the coating are Al and oxygen. Their concentrations in different points change slightly. The coatings are composed mostly of  $Al_2O_3$ , with some content of  $SiO_2$  and  $\gamma-Al_2O_3$ , and  $\alpha-Al_2O_3$  amorphous phase (more details are given in Refs. [7–9]).

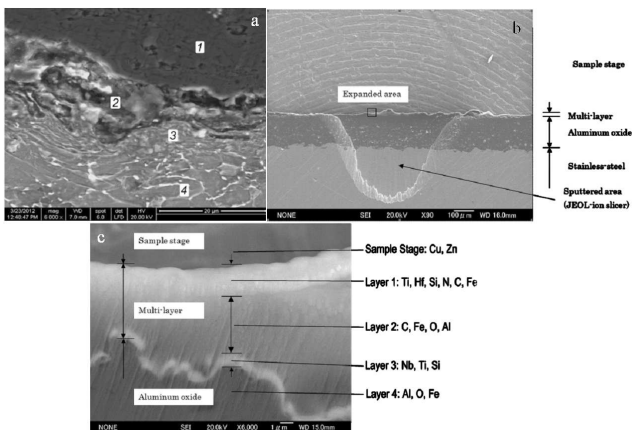


Fig. 1. (a) The structure of the sample coated with  $Al_2O_3$  after etching in a 3% solution of nitric acid. 1 — coating, 2 — transition zone from the coating layer, 3 — transition zone from the substrate, 4 — the base metal (SEM back-scattered electrons mode), (b) cross-sectional images of Ti–Hf–Si–N/NbN/ $Al_2O_3$ -coating (general view), (c) region analysis.

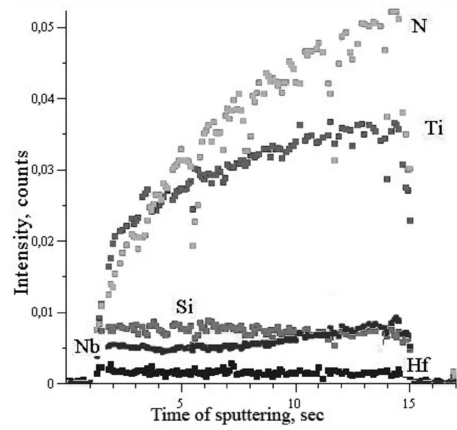


Fig. 2. Data Auger electron spectroscopy from the layers Ti–Hf–Si–N/NbN.

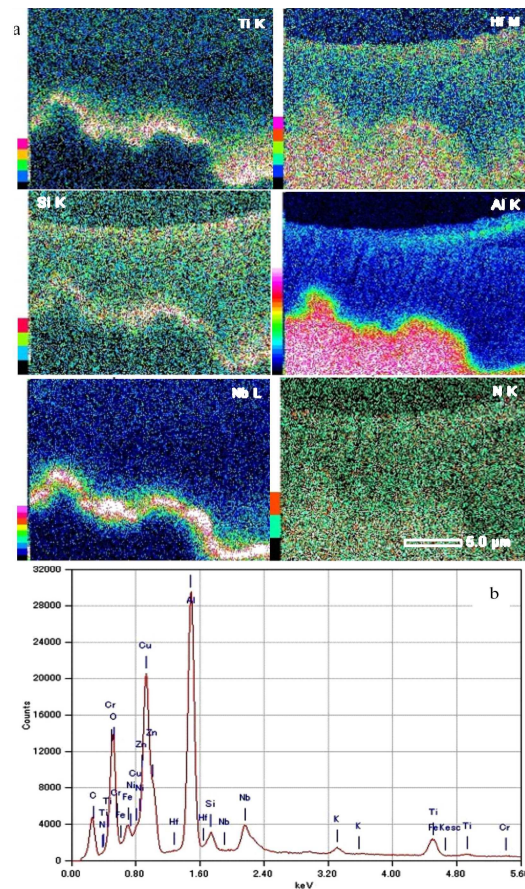


Fig. 3. (a) Coating maps in the elemental contrast, obtained by EDS. (b) Data spectrum of microanalysis for the analyzed area of Ti–Hf–Si–N/NbN/ $Al_2O_3$  multilayered nanocomposite coating.

Figure 1b shows the cross-section of multilayered coatings which was sliced by ion beam. As the figure shows that the total thickness of multilayered coatings is about  $200 \mu m$  (b), the picture below shows the section of the upper part of the multilayered coating. The thickness of the

multilayered coating deposited on the surface of Al<sub>2</sub>O<sub>3</sub>, varied from 5 μm to 12–14 μm due to high roughness of the oxide coating, the value of which after the deposition of powder was about 2.2–8.6 μm.

Figure 2 presents the results of the Auger spectroscopy, which are presented as dependences of element concentration and time of sputtering from the Ti–Hf–Si–N/NbN layers.

The maps in the element contrast made using the energy dispersive spectroscopy (EDS) show that the distribution of elements in the upper layer is homogeneous. However, the concentration of elements is markedly different for different modes (depending on the potential applied to the substrate during the deposition) (Fig. 3a,b). For example, Ti = 28.5 at.%, Hf = 42.2 at.%, Si = 9 at.%

and the rest is N at the potential  $U_{\text{substr}} = -50$  V. At the potential  $-150$  V the concentrations are: Ti = 23.2 at.%, Hf = 38.5 at.%, Si = 7.8 at.%, the rest is N [6].

Measurements of nanohardness  $H$  through the cross-section of multilayered coating showed that its value varied from 47.8 to 56.5 GPa, while the value of elastic modulus ( $E$ ) varied from 435 to 578 GPa. Measurements of nanohardness of the NbN sublayer showed the values from 29.4 to 32.3 GPa, and the lower surface of Al<sub>2</sub>O<sub>3</sub> had hardness  $H$  18.7 to 22.4 GPa. It should be noted that the closer to the transition zone, the hardness is higher. At the same time, the microhardness at a load of 25 g was  $HV_{0.025} = 1525 \pm 25 HV$ . It is also noteworthy that in the transition zone coating/substrate hardness is also much higher than the substrate itself — from 550  $HV_{0.025}$  at the border, to 346  $HV_{0.025}$  in depth.

Tribological characteristics of studied experimental samples.

TABLE

Sample	Friction coefficient ( $\mu$ )		Wear factor [ $\text{mm}^3 \text{H}^{-1} \text{m}^{-1}$ ]	
	At the start	During wear experiment	Counterface [ $\times 10^{-5}$ ]	Substrate [ $\times 10^{-5}$ ]
steel 3	0.204	0.674	0.269	35.36
steel/Al <sub>2</sub> O <sub>3</sub> (200 μm)	0.038	0.959	1.61	22.39
steel/Al <sub>2</sub> O <sub>3</sub> (200 μm)/NbN+TiHfSiN	0.256	0.265	0.184	2.571
steel/Al <sub>2</sub> O <sub>3</sub> (90 μm) cross-section/NbN+TiHfSiN ( $P=0.3$ )	0.02	0.001	4.51	21.43
steel/Al <sub>2</sub> O <sub>3</sub> (90 μm)/NbN+TiHfSiN ( $P=0.8$ )	0.314	0.384	0.936	2.818

Table presents the results of tribological tests. As you can see, the best performance was obtained for the multi-component coatings at a pressure  $P = 0.3$  Pa, where the coefficient of friction in the initial stage was 0.02 and decreased to 0.001 while tested. However, the lowest wear was observed under different conditions of multilayered coatings deposition and it was 0.148 at the counter face, while the sample  $2.571 \times 10^{-5} \text{ mm}^3 \text{H}^{-1} \text{m}^{-1}$ ). The annealing temperature up to 1070 °C in a vacuum about  $10^{-2}$  Pa showed that the coating in the upper layers consists of Ti–Hf–Si–N/NbN. The size of nanograins increases from 25 to 56 nm (for the Ti–Hf–Si–N) and from 14–15 to 35–37 nm for NbN. But on the surface of the upper layer a thin oxide film (thickness 170 nm) formed, which made it impossible for oxygen atoms to penetrate deeper into the coating [7].

### 3. Conclusions

A new type of multi-layer (multicomponent) nano- and microstructured coatings Ti–Hf–Si–N/NbN/Al<sub>2</sub>O<sub>3</sub> with thickness up to 200 μm is presented. It demonstrates high physical-mechanical and tribological properties. Further study of their properties and structure will provide a complete picture of the possibilities of high-performance coatings for protection.

### Acknowledgments

This work was supported by the Ministry of Science and Education, Youth and Sports of Ukraine in the

framework of State program (order No. 411) and NIMS (Tsukuba, Japan), as well as with funding from the Ministry of Education and Science of the Russian Federation in the framework of State contract No. 16.552.11.7087. The authors acknowledge Dr. Yu.N. Tyurin (E. O. Paton Electric Welding Institute, Kiev, Ukraine) and Dr. H. Murakami (National Institute for Materials Science, Tsukuba, Japan) for their help in performance of these experiments.

### References

- [1] J. Musil, J. Sklenka, R. Cerstvy, *Surf. Coat. Technol.* **125**, 322 (2000).
- [2] A.D. Pogrebnjak, A.P. Shpak, N.A. Azarenkov, V.M. Beresnev, *Usp. Fiz. Nauk* **179**, 35 (2009).
- [3] A.D. Pogrebnjak, A.G. Ponomarev, A.P. Shpak, Yu.A. Kunitskij, *Usp. Fiz. Nauk* **182**, 287 (2012).
- [4] A.D. Pogrebnjak, M. Iljashenko, O.P. Kul'ment'eva, V.S. Kshnjakin, A.P. Kobzev, Y.N. Tyurin, O. Kolisnichenko, *Vacuum* **62**, 21 (2001).
- [5] J. Musil, *Surf. Coat. Technol.* **206**, 2105 (2012).
- [6] S. Veprek, *J. Vac. Sci. Technol. A* **17**, 2401 (1999).
- [7] A.D. Pogrebnjak, A.G. Ponomarev, D.A. Kolesnikov, V.M. Beresnev, F.F. Komarov, M.V. Kaverin, S.S. Melnik, *Tech. Phys. Lett.* **38**, 623 (2012).